CONVERGENCE ON MINERAL DETECTIONS OVER GALE CRATER, NE SYRTIS AND JEZERO CRATER USING ADVANCED DATA PROCESSING TECHNIQUES FOR CRISM HYPERSPECTRAL IMAGING DATA. M. Parente[1], R. Arvidson[2], Y. Itoh[1], H. Lin[3], J. F. Mustard[4], A.M. Saranathan[1], F.P. Seelos[5], J. D. Tarnas[4]. [1]Dept. of Electrical and Computer Engineering, University of Massachusetts Amherst, MA 01003 (mparente@ecs.umass.edu). [2]Dept. of Earth and Planetary Sciences, Washington University in St. Louis, St. Louis, MO. [3]Institute of Geology and Geophysics, Chinese Academy of Sciences [4]Dept. of Earth, Environmental and Planetary Sciences, Brown University, Providence, RI. [5]Johns Hopkins University Applied Physics Lab, Laurel, MD.

Introduction: MRO CRISM [1] hyperspectral observations have been central to the selection of landing sites for the Curiosity and Mars 2020 rovers. CRISM has also been used to help define traverse paths for the Opportunity rover to explore smectite-bearing localities on the rim of Endeavour Crater [2,3], to delineate Gale Crater as a landing site due to the presence of smectite and sulfate-bearing strata on Aeolis Mons [4], and to define the Vera Rubin Ridge as a location for a science campaign due to the presence of crystalline hematite [5].

In this work, we compare mineral detections using a number of advanced data processing methodologies, initially focusing on the Curiosity landing site and its traverse areas. We concentrate on overlapping scenes (Table 1) for regions traversed and to be traversed by Curiosity on Mount Sharp, both to provide ground truth observations from the multiple MSL instruments (e.g., [9,10]) to what we retrieve from CRISM data, and to help the rover science team plan future traverse paths. We will also look at overlapping scenes covering NE Syrtis and Jezero (Table 1), with the focus on Jezero in part to provide a collective view of mineralogy expected within the 2020 rover's traverse capabilities.

Table 1: list of images analyzed in this study

Gale	FRT00021C92	FRT0001FD99
HRL0000BABA	FRT0000B6F1	ATO0002EC79
FRT000248E9	FRT0001BBA1	FRT0000C518
Jezero / NE Syrtis	FRT00005C5E	FRT000165F7
HRL000040FF	FRT000161EF	FRT0001642E
FRT00005850	FRT00018DCA	FRS00031442

There is the need to evaluate the veracity and quality of the mapping results if they are to be used in mission critical situations and for science. Our validation consists on defining intrinsic measures of confidence on the mapping results, verifying the quality of the spectra produced by data correction algorithms and the consistency of mineral identifications across overlapping images.

Methods (data correction): The *University of Massachusetts processing pipeline* is featured with a novel atmospheric correction and de-noising method [11], based on the Beer-Lambert law, which automatically learns the atmospheric transmission spectrum and models surface reflectance as a mixture of spectra selected from a large library while noise is simultaneously detected and removed. The effect of water ice aerosols is also considered. The method works on 1.0-2.6 μm region and can be robustly applied to noisy images acquired at high IR detector temperature.

The Washington University (WUSTL) processing pipeline uses the DISORT radiative code to model gases and aerosols for given CRISM scenes, along with the Hapke function for surface scattering, both for solar and mixed solar and emittance at longer wavelengths [6,7,8]. The radiative processing produces single scattering albedo (SSA) spectra (optionally Lambert albedo spectra), and for longer wavelengths surface kinetic temperature maps using neural network approaches. The SSA cubes are then input into a log maximum likelihood processor in which best estimates of signal are retrieved in the presence of either Poisson or Gaussian noise. Data are regularized using spectral and spatial transfer functions with appropriate penalties, and mapped cubes are generated.

Methods (mineral mapping): A mapping technique based on Generative Adversarial networks (GANs) [18] was recently proposed [12]. GANs are a two-neural-network architecture, where one (the generator) is trained to simulate real spectra, the other (discriminator) to distinguish between real and generated spectra. At convergence, one can map the similarity of the discriminator output to each pixel spectrum with respect to the output to a reference mineral spectrum (e.g. from a library). The similarity is a measure of confidence in the mineral identification.

The Dynamic Aperture Factor Analysis/Target Transformation (DAFA/TT) [13] applies factor analysis (via Hysime) [14] and target transformation (FATT) [15] to clusters of ~50 pixels that move across a CRISM image one pixel at a time, applying FATT on each iteration. Factor analysis determines the number of independently varying spectral components from a set of spectra and target transformation performs linear least-squares fitting of independent components to library spectra of minerals [15-17]. DAFA/TT maps the spatial location of minerals within an image by performing FATT in smaller moving windows of differently shaped geometries, and only accepting pixels that are positive detections in all windows.

Results: We present a preliminary study where we apply the combined strength of the four data processing techniques to a set of overlapping images over the

recently proposed alternative paths for the next traverse of the Curiosity rover. Due to the increased spatial fidelity and de-noised spectra produced by the WUSTL processing pipeline [6,7,8] we were able to compute more accurate parameter maps for FRT0000B6F1 (Figure 1, top left). Enhancements in SINDEX2, BD1900 and BD2300 are consistent with the presence of sulfates, hydrous phases and clays. Additional parameters (not shown) indicated high calcium pyroxene (HCP). We used the results of the GAN-based algorithm [12] on images corrected by the Umass pipeline [11] to correlate the parameters with actual maps of mineral distributions (Figure 1, bottom left).

The spectra corresponding to the identified mineral "classes" are reported in Figure 1, right (A to E). We also reported similar identifications in the other overlapping CRISM observations (HRL0000BABA, FRT00021C92 and ATO0002EC79) to verify that the GAN-based algorithm [12] obtained consistent identifications across images on the same locations. The ability of the algorithm in [11] to alleviate the column-dependent "noise" is evident when observing the artifact-free spectral shapes. The spectral plots show in green the spectra from the Mineral Identified through CRISM Analysis (MICA) library [19] used as reference. The system identified (high confidence) Fe-smectites and HCP, a hydrous phase consistent with polyhydrate sulfate (with moderate confidence), confirming a previous identification [20], a hydrous phase that the system attributes with low-to-moderate confidence to analcime, and a phase containing smectite but exhibiting a spectral slope up to 1.8 µm, e.g. a ferrous smectite.

The application of DAFA/TT to the Fe-smectite region of ATO00002EC79 suggested USGS Nontronite NCJB26 as a possible candidate, which corroborates the identification, since NCJB26 is the lab spectrum corresponding to the Fe-smectite MICA reference spectrum.

References: [1] Murchie, S. L. et al. (2007), *J. Geophys. Res., 112,* E05S03, doi: 10.1029/2006JE002682. [2] *Arvidson, R. E. et al. (2014)* Science, *343, doi: 10.1126/science.1248097.* [3] *Fox, V. K., et al. (2016) Geophys. Res. Letters, DOI: 10.1002/2016GL069108.* [4] Milliken, R.E. et al. (2010), *Geophys. Res. Letters, 37, doi:10.1029/2009GL041870.* [5] *Fraeman, A. A., et al. (2013),* Geology, *41, pp. 1103-1106.* [6] *Kreisch, C. D. et al.(2016),* Icarus, *DOI:10.1016/j.icarus.2016.09.033.* [7] He et al., 2019, *50th LPSC*, [8] Politte et al., 2019, *50th LPSC*, [9] Lapotre, M., et al. (2017), *J. Geophys. Res. - Planets*, 10.1002/2016JE005133. [10] Rampe, E. B et al., 2018, *Geophys. Res. Letters*, DOI: 10.1029/2018GL079073. [11] Itoh, Y. and Parente, M. (2019) *50th LPSC*, # 2025. [12] Saranathan, A.M, and Parente, M. (2019) *50th LPSC*, #2698. [13] Lin et al. (2018), *JGR*, in review. [14] Bioucas-Dias, J. M. & Nascimento, J.M.P. (2008) *IEEE Trans. Geo. Rem. Sens.*, 46:8. [15] Malinowski, E.R. (1991) *Fact. Anal. In Chem.* 2nd ed., John Wiley, NY. [16] Amador, E.S. et al. (2018) *Icarus* 311: 113-134. [17] Thomas, N.H. & Bandfield, J.L. (2017) *Icarus* 291: 124-135. [18] Goodfellow, I. et al. (2014) *NIPS,* pp. 2672-2680. [19] Viviano-Beck C. E. et al. (2014) *JGR Planets 119:1403–1431.* [20] Fraeman, A.A et al. (2016), *J. Geophys. Res. – Planets,* 121, doi:10.1002/2016JE005095.

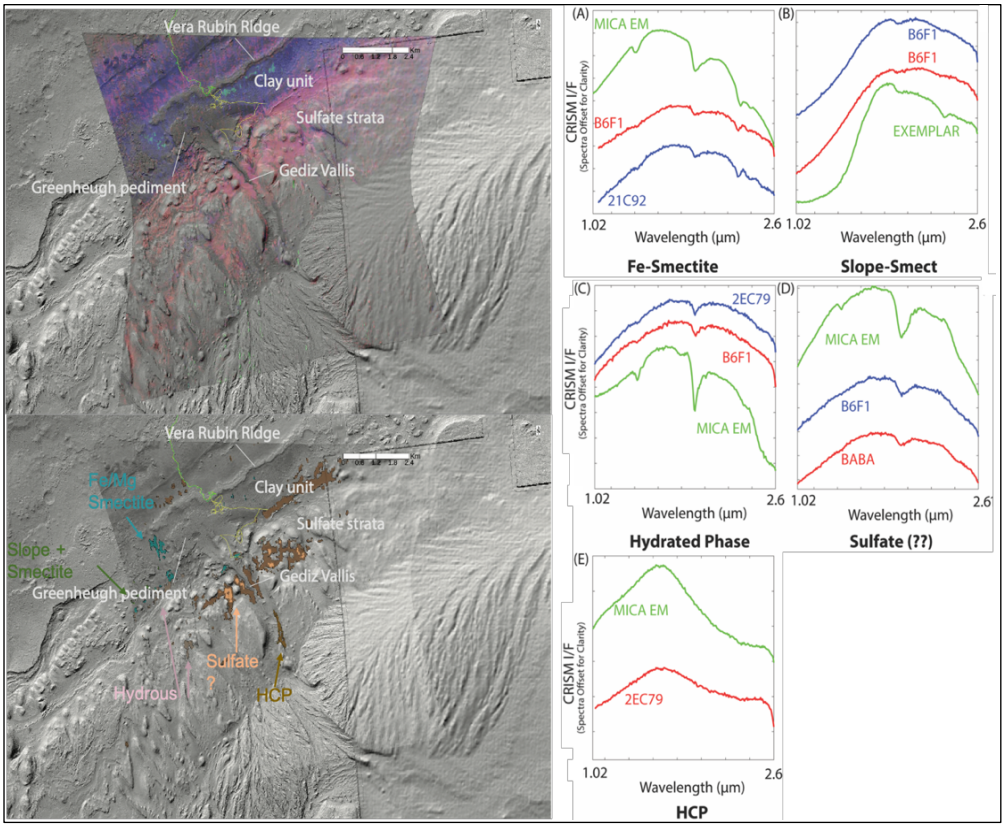

Figure 1: Top left: CRISM parameters (R=SINDEX2, G=2300 nm (smectite) B=1.9 nm (hydrated)) for FRT0000B6F1 over HiRise shaded relief map. Green and yellow paths: current and planned Curiosity traverses. Bottom left: Mineral map of FRT0000B6F1 obtained using [12]. Light/dark brown hydrated phase (consistent with polyhydrated sulfate); Dark orange: HCP; Cyan: Fe smectite, green sloped spectrum + smectite. Right (A to E): examples of detected spectra (in blue and red), reference spectra from the MICA library [19] (in green).